OPEN ACCESS

University of BRISTOL

Rodrigues, S., Barton, D. A. W., Marten, F. B., Kibuuka, M., Alarcon, G., Richardson, Mar, P., & Terry, J. R. (2008). A method for detecting 'ghost' bifurcations in dynamical systems: application to neural-field models.

Link to publication record in Explore Bristol Research
PDF-document

University of Bristol - Explore Bristol Research

General rights

A method for detecting 'ghost' bifurcations in dynamical systems: Application to neural-field models

Serafim Rodrigues, David Barton, Frank Marten, Moses Kibuuka (+),

Gonzalo Alarcon (+), Mark P. Richardson (+) and John R. Terry.

Department of Engineering Mathematics, University of Bristol, BS8 1TR, UK

(+) Institute of Psychiatry, King's College London, De Crespigny Park, London SE5 8AF, UK.

July 31, 2008

Abstract

In this paper we present a method for tracking changes in curvature of limit cycle solutions that arise due to inflection points. We term these changes 'ghost' bifurcations, as they appear to be bifurcations when considering a Poincaré section that is tangent to the solution, but in actual fact the deformation of the solution occurs smoothly as a parameter is varied. These type of solutions arise commonly in EEG models of absence seizures and correspond to the formation of spikes in these models.

1

Tracking these transitions in parameter space allows regions to be defined corresponding to different types of spike and wave dynamics, that may be of use in clinical neuroscience as a means to classify different subtypes of the more general syndrome.

1 Introduction

Many physical and biophysical systems are modelled using *nonlinear dynamical systems* as a means for elucidation and prediction of system behaviour (Schaffer, Kendall and Tidd , 1993). The repertoire of behaviour (solutions) that such systems can display is diverse and includes steady state, periodic and chaotic motion. Transitions between these solutions can occur via many different mechanisms and understanding these transitions is the key to explaining and predicting the process being studied. Bifurcation theory is an important means for understanding transitions that directly affect the nature of the underlying orbits (solutions). These arise when there is a topological change in solution type, upon smooth variation of a system parameter (or parameters). These may modify the orbits *locally* (such as a Hopf bifurcation, or a saddle-node) or

globally (as in a homoclinic or heteroclinic bifurcation). For a more detailed description of such transitions, we refer the reader to (Kuznetsov, Kuznetsov and Marsde , 1998).

Another family of transitions that is of crucial importance in capturing the dynamics of a system is where the geometry of solutions changes upon smooth variation of the parameter. This change in the sign of curvature gives rise to families of orbits, as is the case in *mixed-mode* oscillations, which are oscillatory cycles formed by several small amplitude oscillations followed by a number of large excursions. The presence of mixed-mode oscillations can occur through a variety of mechanisms, for example, via a *delayed-Hopf* bifurcation (Larter, Steinmetz and Aguda , 1988). However, in this case, the pattern of oscillations changes upon smooth variation of a second parameter. In other words, the *delayed-Hopf* bifurcation accounts for the onset of small amplitude oscillations of the mixed-mode orbit but the whole family is obtained through curvature changes by varying an extra parameter.

A further mechanism that results in a change in the sign of the curvature is an *inflection point*, which is the subject of this paper. Specifically, upon smooth variation of system parameter, a periodic oscillation can deform via a sequence

of inflection points, giving rise to different patterns in the solution profile. This behaviour is not exclusive to periodic solutions and has previously been reported for quasiperiodic solutions too (Judd et al., 2008). In this study, the transition is termed *cubic tangency bifurcation*; a reflection of how the trajectory becomes tangent to a Poincaré section at the inflection point. Therein, the focus of study is to characterise mechanisms by which invariant orbits associated with a dynamical system intersect with a varying Poincaré section (i.e. the intersection set changes, but the flow does not). In contrast, our work is concerned with the case where the flow of an invariant orbit changes upon parameter variation without inducing a bifurcation in the traditionally defined manner (Kuznetsov, Kuznetsov and Marsde , 1998). Instead we use the term *ghost bifurcation* to represent a topological change in the intersection set of the Poincaré section with the invariant orbit, that is not a bifurcation of the underlying flow.

When studying delay differential equations (DDEs), that arise naturally in the modelling of biological systems (i.e. in population dynamics or epidemiology) (Baker et al., 1995), it is often the case that several different patterns of (quasi)periodic solutions are observed. Typically the transitions between patterns of activity are not the focus of the study and are generally not characterised or reported (an example of these types of solutions arises in a model of

Hematopoietic regulation (Colijn and Mackey , 2001)). However, recent studies
have demonstrated that transitions in system behaviour via inflection points are
of crucial importance for explaining the onset of spike-wave (SW) activity as
seen in electroencephalogram (EEG) recordings of human brain activity, during
absence seizures (Marten et al., 2008; Rodrigues et al., 2008a).

In this paper, we describe a numerical method that can be used to detect
such transitions as an add-on to the numerical continuation package, DDE-
BIFTOOL (Engelborghs, Luzyanina and Samaey , 2001). DDE-BIFTOOL is a
Matlab package that can detect the onset and termination of bifurcations and
follow solutions in parameter space for systems of DDEs, in a similar manner
to the package AUTO (Doedel et al., 1998) for ODEs.

2   Description of the method

We focus on delay equations with a single fixed delay which may be represented
as follows:

$$
\begin{cases}
\dot{x} = f(x(t), x(t-\tau), \nu), & t > 0 \\
x(t) = \varphi(t), & t \leq 0.
\end{cases}
\tag{1}
$$

Here f is a continuously differentiable vector field in an n-dimensional state
space, $\tau \in \mathbb{R}$ is the fixed delay, while $\nu \in \mathbb{R}^p$ represents a number of control

parameters and the functional component $\{x(t-\tau), -\tau < t-\tau < 0\}$ represents past states. The existence of a unique solution requires a function (*history*) as initial data on the interval $[-\tau, 0]$, i.e $\varphi : [-\tau, 0] \to \mathbb{R}^n$. The presence of the history function implies that the phase space of the system is an infinite dimensional space consisting of functions with values in the state space $\mathbb{R}^n$. Denoting this infinite dimensional space as $\mathcal{C}$, then $\varphi \in \mathcal{C}$ and the evolution operator is now defined as $\Phi^t(\varphi) : \mathcal{C} \to \mathcal{C}$. This describes how the initial conditions $\varphi \in \mathcal{C}$ evolve in time with the solution given by a vector valued function $x(t) : [0, \infty) \to \mathbb{R}^n$. We now proceed to describe the formulation of our problem in a framework suitable for numerical continuation, which employ techniques for periodic-boundary value problems (P-BVP).

2.1   Periodic orbits as a periodic-boundary value problem

Mathematically, we define the inflection point criteria for a P-BVP as follows:

$$\begin{cases} \dot{x} = Tf(x(t), x(t - \tau/T \mod T), \nu), \\[2mm] x(0) = x(1), \\[2mm] \frac{\partial f_1(x(1), x(1-\tau/T), \nu)}{\partial t} = \frac{\partial^2 f_1(x(1), x(1-\tau/T), \nu)}{\partial t^2} = 0. \end{cases} \tag{2}$$

Here we have rescaled the vector field, $f(.)$, so that its time scale, corresponds to that of period T, giving the term $x(t - \tau/T)$. The parameter, T, is the period of oscillation as determined by the boundary value problem. The periodicity condition is given by $x(0) = x(1)$, that is periodic oscillations are rescaled

to the time interval $[0, \ 1]$. The final equation defines the conditions for an inflection to occur on the first component of the vector field, that is, f_1. To numerically solve (2), a discretisation scheme is required for which we use the *collocation method* as follows.

Collocation is a theoretical framework that enables the discretisation of solutions of a differential equation defined on some continuous function space X. This discretisation replaces X with a finite-dimensional space X_N which discretises the set of differential equations. In particular, the method uses orthogonal piecewise polynomials (in space X_N) to approximate the solution defined by the P-BVP. This is achieved by ensuring that the set of piecewise polynomials satisfies the underlying differential equation at a set of discrete *collocation points* (Doedel, Keller and Kernevez , 2005; Engelborghs el al., 2001). When this set of piecewise polynomials are substituted into the P-BVP and evaluated at the collocation points, a large system of nonlinear algebraic equations is obtained which can be solved using standard root-finding methods, such as Newton iteration. In addition, solutions satisfying a P-BVP can be mapped out in parameter space using *numerical continuation*, which is a technique adopted in bifurcation analysis packages, such as AUTO and DDE-BIFTOOL (Engelborghs, Luzyanina and Samaey , 2001). To make these ideas clearer, we proceed to describe this method in more detail.

Let L represent the number of collocation intervals and let m denote the number of subintervals within each collocation interval. We define a partition Π as a set of $mL + 1$ mesh points over the range $[0, 1]$, given by:

$$\Pi := t_0 = 0 < \cdots < t_j < \cdots < t_{j+i/m} < \cdots < t_{j+1} < \cdots < t_L = 1, \quad (3)$$

for integer values $j = \{0, \cdots, L - 1\}$ and $i = \{0, \cdots, m\}$. The collocation solution $x(t)$ lies on the interval $[0, 1]$ and is a piecewise vector-valued polynomial, defined on the mesh Π, of the form:

$$x \in \mathcal{C}([0, 1], \mathbb{R}^n), \quad x|_{[t_j, t_{j+1}]} \in P^m. \quad (4)$$

Here P^m is the set of all (vector-valued) polynomials with degree at most m.

To fix the solution, we require values of $x(t)$ at $n(mL + 1)$ points, chosen appropriately in time and we assume continuity of the collocation solution at the boundaries of the collocation intervals. In particular, the collocation solution $x(t)$ is given by a piecewise polynomial function represented in the Lagrange form:

$$L_{j,i}^m(t) = \sum_{i=0}^{m} \ell_{j,i}(t) x_{j+i/m}, \quad t \in [t_j, t_{j+1}] \quad (5)$$

where $x_{j+i/m}$ samples the solution profile $x(t)$ and the polynomial basis, ℓ,

consists of the Lagrange polynomials:

$$\ell_{j,i}(t) = \prod_{k=0, k \neq i}^{m} \frac{t - t_{j+k/m}}{t_{j+i/m} - t_{j+k/m}}. \tag{6}$$

such that ℓ satisfies the Kronecker-delta function (i.e. $l_{j,i}(t_{j+i/m}) = 1$ and $l_{j,i}(t_{j+k/m}) = 0 \ \forall k \neq i$). Specifically for convergence of the solution within each of the subintervals $[t_j, t_{j+1}]$, the mesh points $t_{j+i/m}$, are chosen to be the roots of the Legendre polynomials (denoted here as $z_{j,i}$). This enables us to numerically calculate $n(mL+1)$ approximants, $x_{j+i/m}$, that tend to $x(t)$ in an optimal manner when the mesh interval tends to zero. In fact in the case of ODEs the approximants tend to the solution with point-wise superconvergence at the boundary of each collocation interval (Engleborghs and Doedel , 2002). Furthermore, the resulting piecewise polynomials $L_{j,i}^m(t)$ satisfy the system of mL vector-valued equations:

$$\dot{L}_{j,i}^m(z_{j,i}) - f(L_{j,i}^m(z_{j,i}), L_{j,i}^m(z_{j,i} - \tau/T), \nu) = 0. \tag{7}$$

Note that while the collocation solution is continuous for $t \in [0, 1]$ it may not be continuously differentiable at the boundaries of each collocation interval. A schematic of this collocation method is illustrated in Fig (1).

2.2 Detection of inflection points

Suppose that a periodic solution, $\gamma(t)$, satisfying the DDE (1) is found either via numerical integration or continuation, then we can use the P-BVP (2)

9

to investigate whether the solution satisfies the inflection point criteria. To achieve this, both the P-BVP (2) and $\gamma(t)$ are appropriately discretised using the collocation method and then the solution is evaluated using a Newton iteration scheme as shown in Figure (1). Importantly, the P-BVP (2) has to be well posed and the initial orbit, $\gamma(t)$, has to be close enough to the true solution (with inflection point), $x(t)$, to ensure convergence of the Newton method. Once $x(t)$ is found, it is then possible to follow it in parameter space using standard continuation methods. To set up a well posed P-BVP, we need to match the number of equations with the number of unknowns and these may be either variables or parameters. In addition, it is required that at least one parameter from equation (1) is free, so as to enable a solution to be found.

In particular, we observe that the P-BVP (2) has at least $n+2$ unknowns. There are n values corresponding to the physical dimension of the delayed equation (1), an unknown period, T, and at least one parameter, $\nu_l \in \nu$, that is allowed to vary; hence in total at least $n + 2$ unknowns. To guarantee uniqueness of the solution, $x(t)$, it must satisfy $n + 2$ boundary conditions in order to be a well posed P-BVP. From P-BVP (2) we note that we have n point-wise periodic boundary conditions corresponding to the condition $x(0) = x(1)$ and two extra conditions corresponding to the inflection point criteria, $\frac{\partial f_1(.)}{\partial t} = 0$ and $\frac{\partial^2 f_1(.)}{\partial t^2} = 0$, giving a total of $n + 2$ boundary conditions.

10

It is worth mentioning that in general, a *phase condition* is required by continuation methods to guarantee a unique periodic solution in a well posed P-BVP. An example of *phase condition* is one that minimises the distance between two periodic orbits, $\min_{\theta}\{\int_0^1 ||x(t + \theta) - x(t)||\}$. However, we replace the *phase condition* by a *Poincaré phase condition* (i.e. inflection point criteria) which provides the required $n + 2$ boundary conditions to guarantee uniqueness of solutions. Hence, we may consider the whole method as a functional that acts on the vector field (dynamical system) and detects an inflection point and once converged onto this inflection point, it is then possible to trace it in parameter space.

2.3 Illustration of the method

To illustrate the detection method we consider a model of cortico-thalamic interactions (as studied for example in (Marten et al., 2008)) and use the software package DDE-BIFTOOL. To this package, we provide relevant MATLAB code as an add-on for the detection of ghost bifurcations as outlined in the previous section. The procedure for the detection of a ghost bifurcation is similar to the principles outlined in the user manual of DDE-BIFTOOL for the detection of true bifurcations. The source code for this may be found at (Rodrigues et al., 2008b).

The specific model that we use to illustrate the method was recently proposed to explain the existence of (poly)spike-wave activity, as observed in electroencephalogram (EEG) recordings of human brain activity, during absence seizures (Marten et al., 2008), which may be written as follows:

$$
\begin{cases}
\frac{d}{dt}\phi_e(t) = y(t), \\[2mm]
\frac{d}{dt}y(t) = \gamma_e^2\left[-\phi_e(t) + \varsigma(V_e(t))\right] - 2\gamma_e y(t), \\[2mm]
\frac{d}{dt}V_e(t) = z(t), \\[2mm]
\frac{d}{dt}z(t) = \alpha\beta\left[-V_e(t) + \nu_{ee}\phi_e(t) + \nu_{ei}\varsigma(V_e(t)) + \nu_{es}\varsigma(V_s(t))\right] - (\alpha+\beta)z(t), \\[2mm]
\frac{d}{dt}V_s(t) = w(t), \\[2mm]
\frac{d}{dt}w(t) = \alpha\beta\left[-V_s(t) + \nu_{sn}\phi_n + \nu_{se}\phi_e(t) + \nu_{sr}^A\varsigma(V_r(t)) + \nu_{sr}^B\varsigma(V_r(t-\tau))\right] - (\alpha+\beta)w(t), \\[2mm]
\frac{d}{dt}V_r(t) = v(t), \\[2mm]
\frac{d}{dt}v(t) = \alpha\beta\left[-V_r(t) + \nu_{re}\phi_e(t) + \nu_{rs}\varsigma(v_s(t))\right] - (\alpha+\beta)v(t).
\end{cases}
\tag{8}
$$

The principal state variable, ϕ_e (cortical mean-field), is the only observable of interest, as it relates directly to EEG. The control parameters of interest are, ν_{se}, and the delay, τ. For a complete description of the model, as well as details of other parameters we refer the reader to (Marten et al., 2008). An exemplar of absence seizure data with (poly)spike-wave is depicted in Fig (2).

A plot of a noise free bifurcation diagram showing a transition from steady state to limit cycles is shown in Figure (3-a). The bifurcation diagram is obtained by numerically simulating the system, allowing transients to decay, and then

12

plotting the local maxima and minima of the amplitude of the principal state variable, ϕ_e, as we increase the parameter of interest, ν_{se}. Beyond the Hopf bifurcation extra structures that appear to be bifurcations appear for parameter values between $\nu_{se} \approx 1.5 \times 10^{-3}Vs$ and $\nu_{se} \approx 1.7 \times 10^{-3}Vs$ and also between $\nu_{se} \approx 1.8 \times 10^{-3}Vs$ and $\nu_{se} \approx 1.9 \times 10^{-3}Vs$. However, DDE-BIFTOOL does not highlight these transitions points as bifurcations. It turns out that at these parameter values the solutions develop a local maximum via an inflection point, the ghost bifurcation, that we described previously. To confirm this, we start with any periodic solution beyond the Hopf bifurcation and close enough to the ghost bifurcation point of interest. The solution can either be obtained from a numerical simulation for a fixed parameter value of ν_{se}, which is then discretised using a collocation scheme. Alternatively, the solution can be obtained via a continuation process in DDE-BIFTOOL by tracing out branches of periodic orbits emanating from the Hopf bifurcation. Any periodic solution computed can be taken as initial guess for the Newton's scheme, which makes use of the inflection P-BVP (2). The add-on to DDE-BIFTOOL then iterates through parameter space, ν_{se} and detects ghost bifurcations as shown in Figure (3-b). The middle inset of figure (3-b) shows a convergence to a periodic solution satisfying the P-BVP (2). This procedure can be repeated for other nearby solutions satisfying the inflection point criteria. In addition, it is possible to

13

trace the locus of these solutions in two parameter space by making use of DDE-BIFTOOL's continuation methods as shown in figure (4). This Figure presents the onset of solution types which can then be used to classify or predict a system's behaviour. In particular, Figure (2) shows that complex patterns of periodic solutions can arise depending on the number of ghost bifurcations points past. Indeed, it is possible for the coexistence of two or more inflection points as shown in Figure (4). Finally, the method fails to converge when a ghost bifurcation point collides with a true bifurcation points. However, it is possible to adapt the method to allow the detection of an inflection point, even when a bifurcation is encountered, which is the subject of future developments.

3 Discussion

In this paper, we introduce the concept of a ghost bifurcation; that is a transition that appears to occur as a result of a bifurcation, when considering a Poincaré Section that is tangential to the flow of a dynamical system, but in actual fact arises as a result of an inflection point in the flow. Using the software package DDE-BIFTOOL we have developed an add-on for detecting these ghost bifurcations points and illustrate how they correspond to the formation of 'spikes' in a DDE model of human EEG. The detection of 'spikes' is key to understanding the transitions to spike-wave activity in EEG models of absence

seizures and mapping these transitions in parameter space provides a means to classify absence seizure data. In this way, a more detailed clinical study of absence seizure could be performed. It should be noted that absence seizures have not been clinically reported to have subtypes syndromes. However, it is known that absence seizures can arise via different physiologic mechanisms within a cortico-thalamic pathway and absence EEG data vary from subject to subject. This suggests, that variants of these disease should be identified and thus ought to be considered as a subject of further investigation. The EEG models of absence seizures we have developed and the methodology presented in this paper can provide a root to categorising the disease. For example, classifying various subtypes of absence epilepsies could be achieved by performing parameter fitting of the above cortico-thalamic model (8) from absence EEG data and determining in what region of parameter space, as shown in Fig (4), the seizure lies.

4 Acknowledgment

References

Baker, C. T. H., Paul, C. A. H., Willé, D. R. (1995) A bibliography on the numerical solution of delay differential equations. *Numerical Analysis Report 269, Mathematics Department, University of Manchester, U.K.*

Breakspear, M., Roberts, J. A., Terry, J. R., Rodrigues, S., Mahant, N., Robinson, P. A. (2006) A unifying explanation of primary generalized seizures through nonlinear brain modeling and bifurcation analysis. *Cerebral Cortex* 16:1296–1313.

Colijn C., Mackey, M. C. (2001) Bifurcation and Bistability in a Model of Hematopoietic Regulation. *SIAM J. App. Dyn. Sys.* 6:378–394.

Doedal, E., Keller, H., Kernevez, J. (2005) Numerical analysis and control of bifurcation problems, Part II. *International Journal of Bifurcation and Chaos* 1(14):745–772.

Doedel, E., Champneys, A., Fairgrieve, T., Kuznetsov, Y., Standstede, B., Wang, X. (1998) AUTO 97: Continuation and bifurcation software for ordinary differential equations *http://indy.cs.concordia.ca/auto/*.

Engelborghs, K., Luzyanina, T., In 't Hout, K. J., Roose, D. (2001) Collocation methods for the computation of periodic solutions of differential equations. *SIAM Journal on Scientific Computation* 22(5):1593–1609.

Engelborghs, K., Luzyanina, T., Samaey, G. (2001) DDE-BIFTOOL v-2.00. A Matlab package for bifurcation analysis of delaly differential equations. *Technical Report TW330, Department of Computer Science, K. U. Leuven Belgium.*

Engelborghs, K., Doedel, E. (2002) Stability of piecewise polynomial collocation for computing periodic orbits of delay differential equations. *Numerische Mathematik* 91:627–648.

England, J. P., Krauskopf, B., Osinga, H. M. (2005) Computing One-Dimensional Global Manifolds of Poincaré Maps by Continuation. *SIADS* 4(4):1008–1041.

Judd, C. M., Collins, P. J., Krauskopf, B., Osinga, H. M. (2008) Tangency bifurcations of global Poincaré maps. *to appear in SIAM Journal on applied dynamical systems.*

Koper, M. (1995) Bifurcations of mixed-mode oscillations in a three-variable autonomous van der Pol-Duffing model with a crossed-shaped phase diagram. *Physica D* 80:72–94.

Krupa, M., Popović, N., Kopell, N., Rotstein, H. G. (2008) Mixed-mode oscillations in a three time-scale model for the dopaminergic neuron. *Chaos* 18:015106.

Kuznetsov, Y., Kuznetsov L., Marsde, J. (1998) Element of Applied Bifurcation Theory *Springer-Verlag, New York*.

Larter, R., Steinmetz, C., Aguda, B.. (1988) Fast-slow variable analysis of the transition to mixed-mode oscillations and chaos in the peroxidase reaction. *J. Phys. Chem.* 89:6506-6514.

Larter, R., Steinmetz, C. (1991) Chaos via mixed-mode oscillations. *Phil. Trans. R. Soc. Lond. A* 337:291–298.

Marten, F., Rodrigues, S., Benjamin, O., Richardson, M. P., Terry, J. R. (2008) Onset of poly-spike complexes in a mean-field model of human EEG and its application to epilepsy. (to appear in Phil. Trans. Royal Soc. Volume A).

Rodrigues, S., Terry, J. R., Breakspear, M. (2006) On the gensis of spike-wave activity in a mean-field model of human thalamic and cortico-thalamic dynamics. *Physics Letters A* 355:352–357.

Rodrigues, S., Barton, D., Szalai, R., Benjamin, O., Richardson, M. P., Terry, J. R. (2008) Transitions to spike-wave oscillations and epileptic dynamics in a human cortico-thalamic mean-field model. (submitted to J. Comp. Neurosci.).

Rodrigues, S., Barton, D., Szalai, R., Benjamin, O., Richardson, M. P., Terry,

J. R. (2008). Inflection point periodic boundary value problem: Source code: `http://seis.bris.ac.uk/~enxsr/code.html`.

Schaffer, W. M, Kendall, B. E., Tidd, C. W. (1993) Transient periodicity and episodic predictability in biological dynamics. *IMA J. Mathematical Med. and Biol.* 10:227–247.

Thota P. (2007). Analytical and Computational Tools for the Study of Grazing Bifurcations of Periodic Orbits and Invariant Tori. *PhD. Thesis, Faculty of the Virginia Polytechnic Institute and State University*.
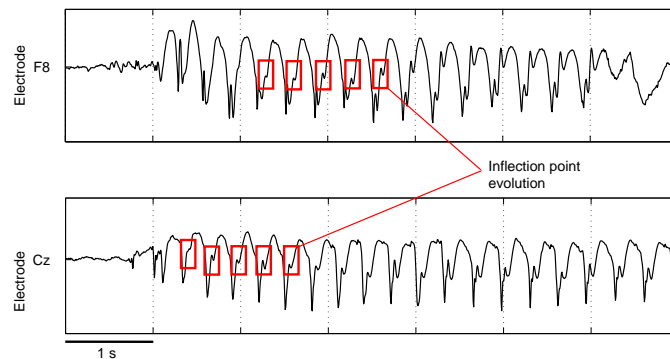
Figure 1: *Scalp EEG from human subjects with childhood absence epilepsy. The traces represents aggregate brain electrical activity, in this case recorded from electrodes $F8$ and Cz. The seizure is marked by the large amplitude oscillations that are periodic, approximately three oscillations per second, which arise due to increased spatial and temporal coherence in the EEG. In particular, these seizures are characterised by spike and wave morphology on each cycle. The spike component appears to evolve during the initial cycles (e.g. see the left red boxes) and increases smoothly in amplitude over time. In addition, the amplitude of the spikes can remain relatively constant (with small variations) or vanish reflecting an underling dynamics that occurs simultaneously to the one that causes periodic waves. Via mathematical modelling of absence epilepsy (Marten et al., 2008; Rodrigues et al., 2008a) we investigated the appearance and anhilation of spikes and we explain that these arise as a result of an inflection point of the vector field.*
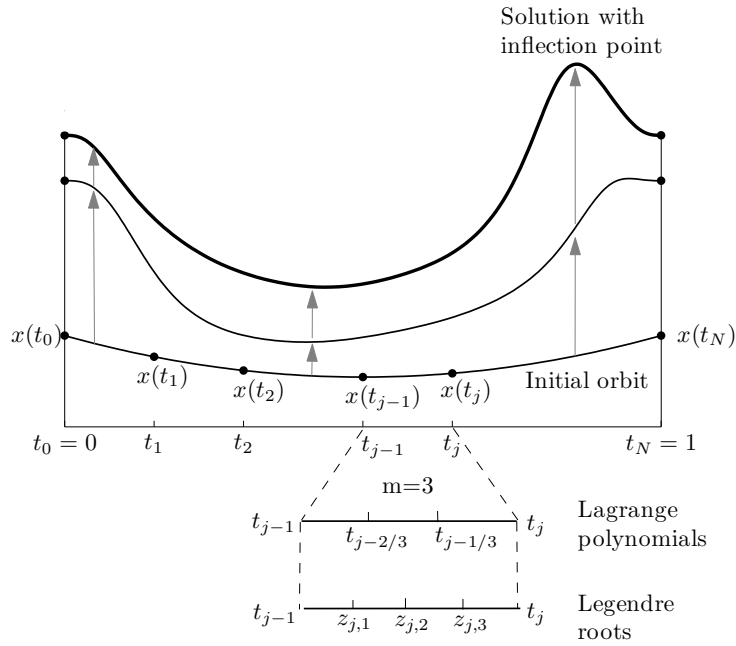
20

Figure 2: *A sketch adapted from (Thota , 2007) which illustrates the collocation scheme. A periodic trajectory is represented by mesh points within the interval $[0,1]$. Trajectories are appropriately discretised and represented by a piecewise polynomial in Lagrange form given by equation (5). In this instance, the initial periodic orbit corresponds to the lower parabolic curve, which is then evaluated (vertical gray arrows) via Newton's method until it converges to a solution with an inflection point. Both the initial and final orbit satisfy the delay differential equation through the algebraic equation (7), which allows to test at every Newton step the trajectories of the model against the inflection point criteria defined by the periodic boundary value problem (2). In this particular implementation, we test the inflection point conditions on one of the boundaries of the mesh interval, e.g. at $t_N = 1$. To ensure convergence, the collocation scheme relies on Legendre roots.*
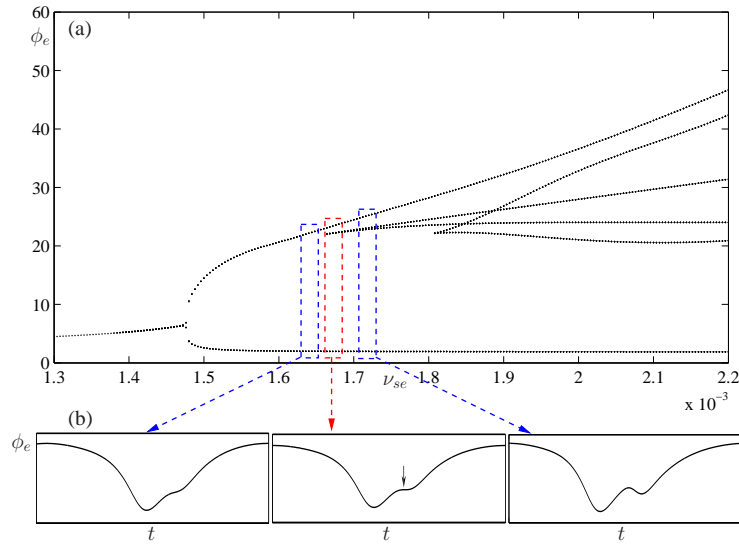
Figure 3: *From the system of equations (8), we generate numerically a bifurcation diagram in the variable ϕ_e, versus the parameter ν_{se}, illustrated in part (a). The bifurcation diagram was achieved by plotting the local maxima and local minima of the solution profiles obtained through numerical simulations. In part (b), we show three different solution profiles of the model. Starting from a nearby solution, for example the solutions in the regions of the dashed boxes corresponding to the blue dashed arrows, converge by Newton's scheme to the ghost bifurcation point in the middle box (as shown by the red dashed arrow). The black arrow in part (b) indicates the inflection point.*
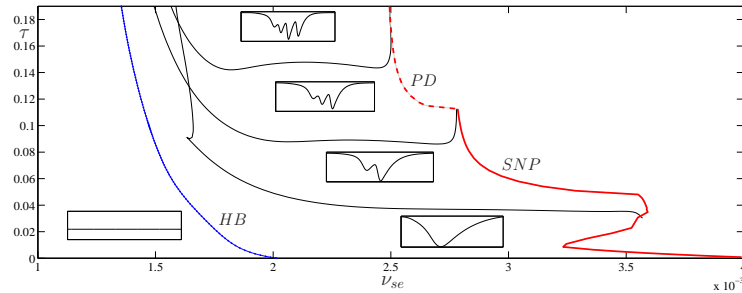
Figure 4: *Illustrating a two parameter continuation diagram, containing both branches of true bifurcations, as well as ghost bifurcations, demonstrating how different regions correspond to different solutions of the original system (8). The blue line corresponds to a branch of Hopf bifurcations, HB, corresponding to a transition from steady-state to periodic behaviour. The dashed red line corresponds to the onset of period-doubling bifurcations, PD and the red solid lines to the birth of saddle-node of periodic orbits, SNP. The black lines correspond to branches of ghost bifurcation points, i.e. deformation of the solutions due to inflection points. It should be noted, that the iteration fails to converge onto a ghost bifurcation point, when it collides with the onset of a true bifurcation, for example, PD and SNP as depicted in the Figure. The inset figures show different solution profiles arising due to different number inflection points, which provides a means for the generation of complicated patterns in the model.*